Supplement of Hydrol. Earth Syst. Sci., 29, 6735–6760, 2025
https://doi.org/10.5194/hess-29-6735-2025-supplement

Hydrology and Earth System Sciences
Open Access
EGU

Supplement of

Technical note: An illustrative introduction to the domain dependence of spatial principal component patterns

Christian Lehr and Tobias L. Hohenbrink

Correspondence to: Christian Lehr (christian.lehr.1@uni-potsdam.de)

Supplements

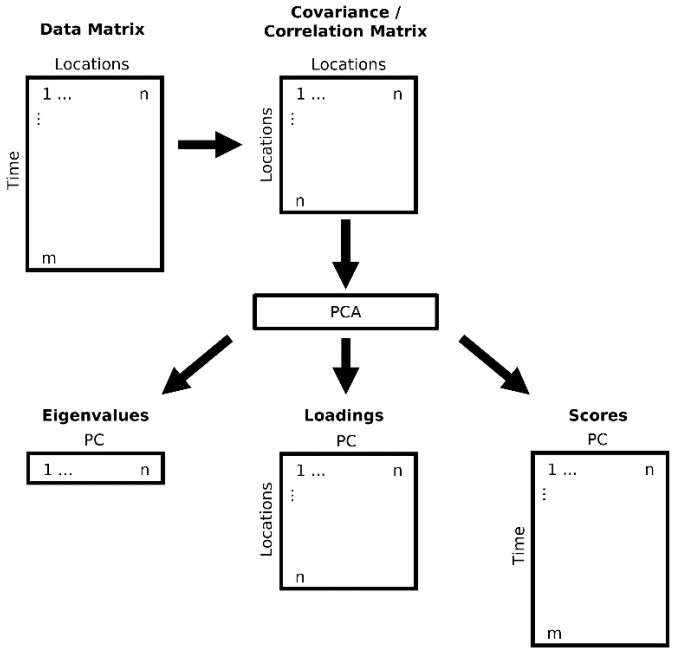

Figure S1 S-mode PCA, adapted after Figure 9 in Richman (1986). n: number of locations, m: number of time steps. The eigenvalues define the explained variance, the loadings the unscaled spatial PC patterns and the scores the temporal PC patterns.

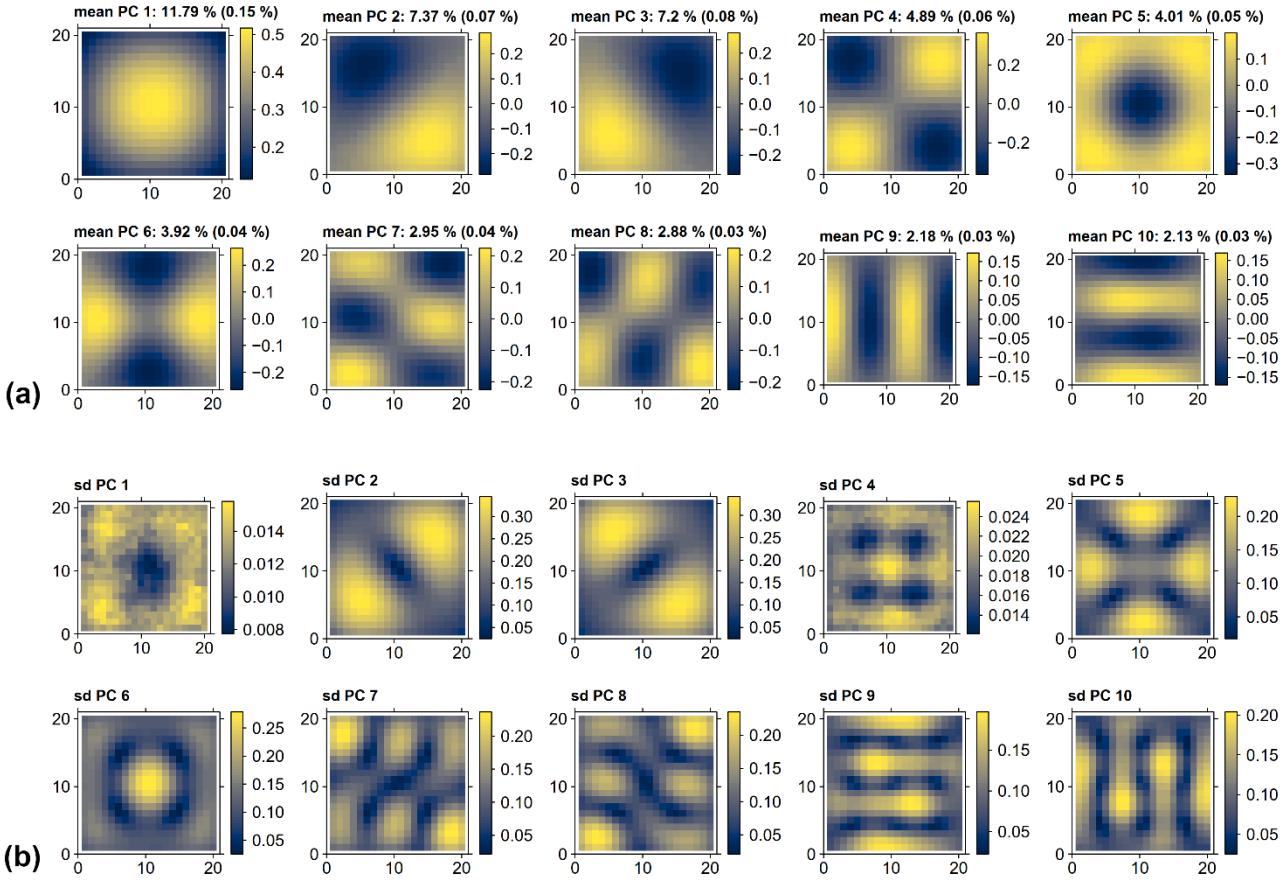

Figure S2 Detail plot of mean (a) and standard deviation (b) of the spatial patterns from the leading ten PCs of the data set ensemble with the square domain shown in Figure 8a and Figure 9a. The panel titles of (a) contain the mean (and standard deviation) of the percentages of variance assigned to the respective PCs from the 100 PCAs of the ensemble.

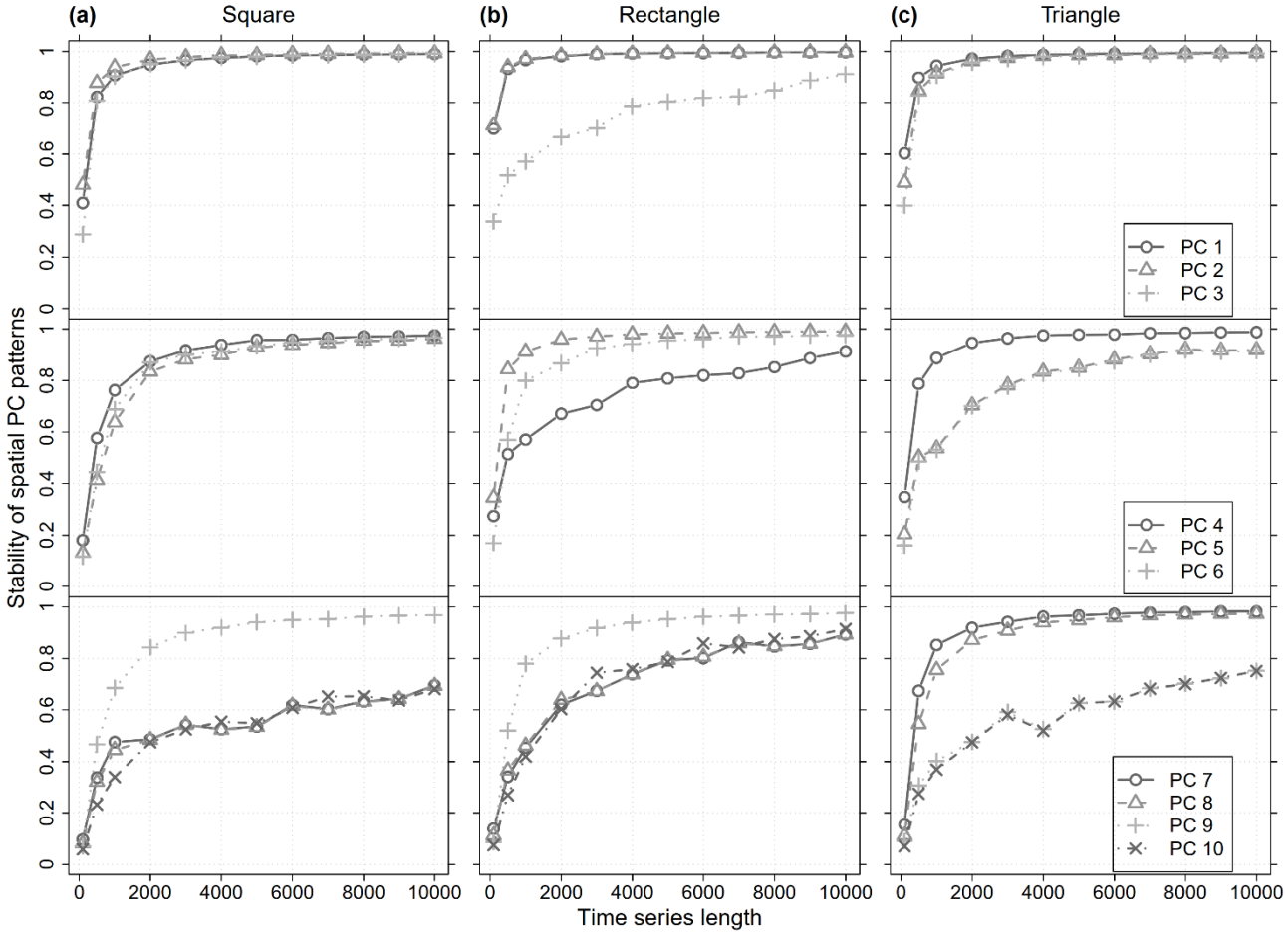

Figure S3 Stability of the spatial PC patterns as in Figure 7 but for the patterns of the Het40 variant (Figure 11). The stability is measured by the mean R^2 of the correlation between the spatial patterns of all PCs with identical rank derived from an ensemble of 100 data sets simulated with the respective time series length. For details see the caption of Figure 7.

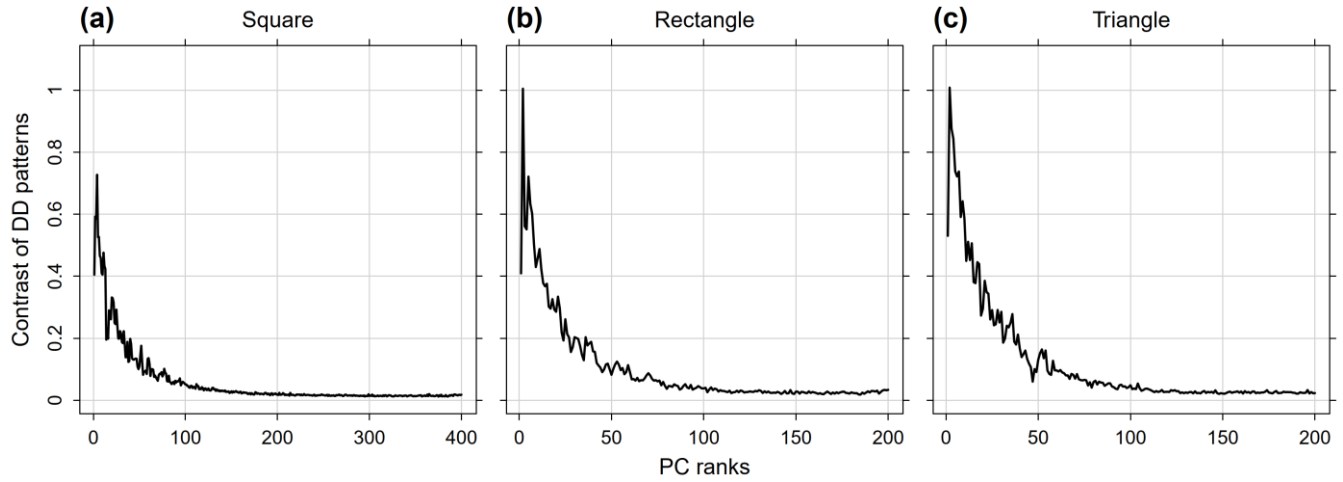

Figure S4 Contrast of all DD patterns modelled with the analytic DD reference method using an isotropic exponential covariance model, spatial correlation length of 10 cells and the domain boundaries (a) square, (b) rectangle and (c) triangle from Figure 6. All cells within the boundaries were used. Note that the number of PCs depends on the number of analysed series, which equals here the number of cells in the domains.

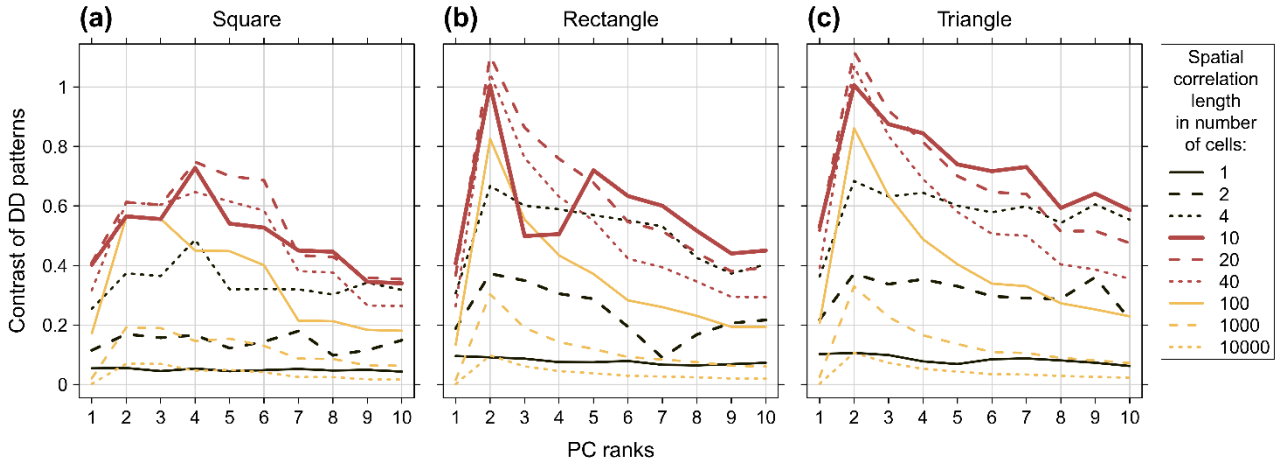

Figure S5 Contrast of the ten leading DD patterns PCs modelled with the stochastic DD reference method using an isotropic exponential covariance model, nine different spatial correlation lengths and the domain boundaries (a) square, (b) rectangle and (c) triangle from Figure 6. All cells within the boundaries were used. For each correlation length, the DD reference patterns were estimated from ensembles with 100 simulated data sets, each with time series length 10 000.

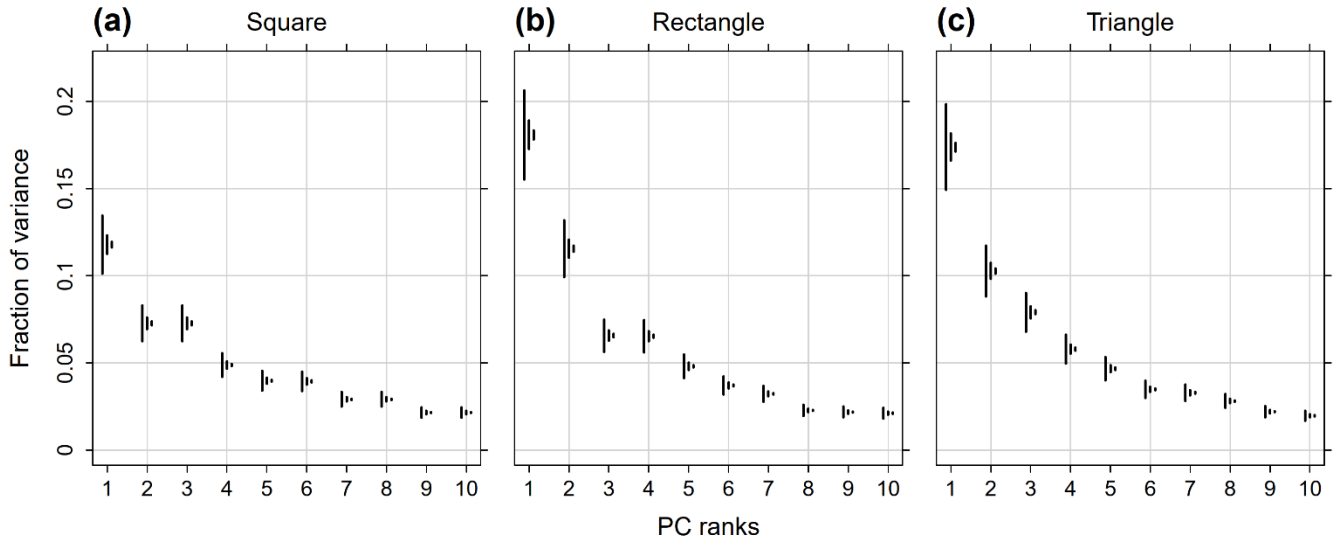

Figure S6 Variance representation of the ten leading PCs modelled with the analytic DD reference method using an isotropic exponential covariance model, a spatial correlation length of 10 cells and the domain boundaries (a) square, (b) rectangle and (c) triangle from Figure 6. All cells within the boundaries were used. The upright bars show from left to right the 95 % confidence interval for an effective sample size of 100, 1 000 and 10 000 estimated with North´s rule of thumb (North et al., 1982; Hannachi et al., 2007). For time series without temporal autocorrelation the effective sample size equals the time series length.

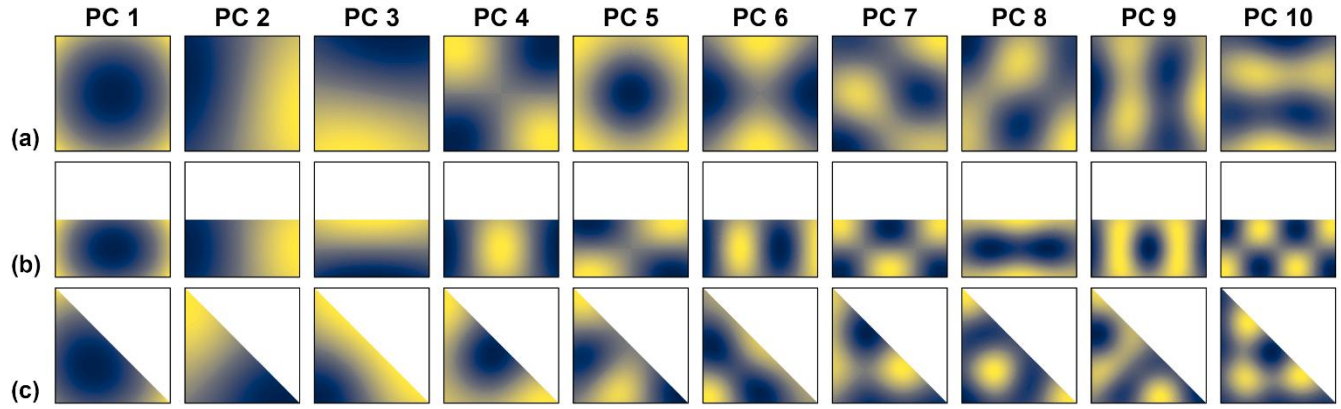

Figure S7 Overview of the ten leading DD reference patterns for the spatial PC patterns of the precipitation data sets from Figure 16. In each subplot, the colour gradient depicts from blue to yellow the range between the minimum and maximum values of the respective spatial pattern. The patterns were estimated with the analytic method with an isotropic spherical covariance model and a spatial correlation length of 770 km. For comparison: The mean range of the spherical sample variograms from all 360 monthly 200 km × 200 km square precipitation raster (Figure 3) was 824 km. The sample variograms were estimated with the R package "gstat" using the default settings and the cut off length set to the side length of the square.

	PC 1	PC 2	PC 3	PC 4	PC 5	PC 6	PC 7	PC 8	PC 9	PC 10
Square	80.02	5.68	5.68	1.24	0.99	0.80	0.44	0.44	0.29	0.29
Rectangle	84.52	6.71	2.24	1.28	0.76	0.48	0.37	0.28	0.21	0.20
Triangle	84.08	6.25	3.02	1.25	0.75	0.47	0.43	0.33	0.22	0.20

Table S1 Percentages of assigned variances from the DD reference for the precipitation PCAs (Figure S7).

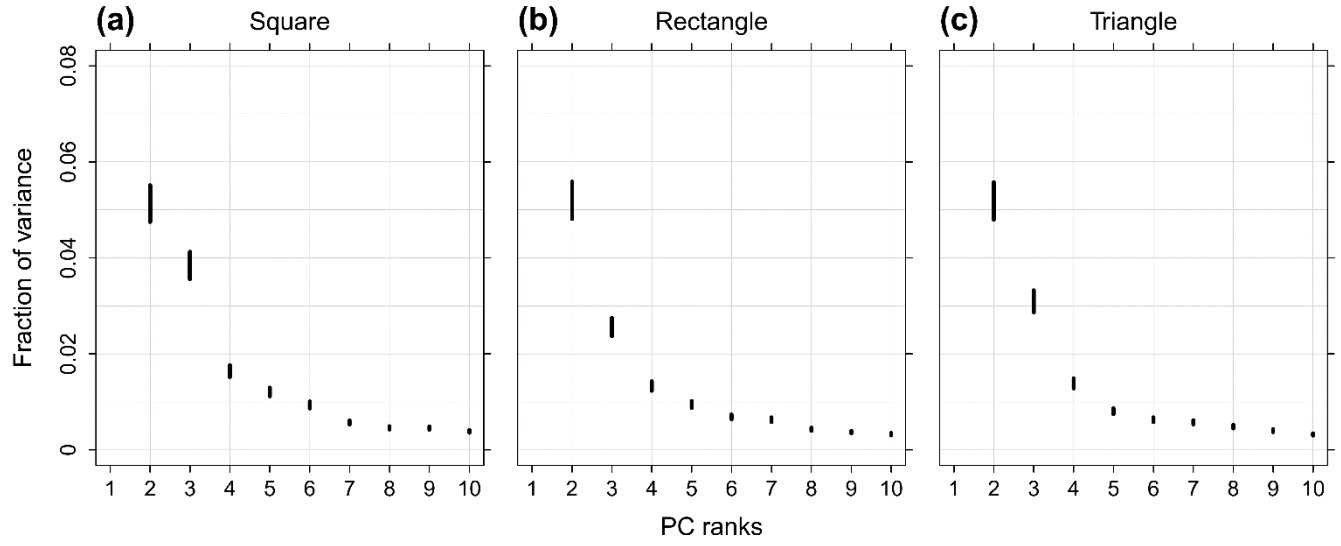

Figure S8 Separation of the leading PCs from the precipitation PCAs (Table 3). The upright bars show the 95 % confidence interval estimated with North´s rule of thumb (North et al., 1982; Hannachi et al., 2007) and an effective sample size of 360 (the time series lengths of the precipitation data sets). In all three domains, the first PC is substantially larger than the other PCs and clearly separated from them. Therefore, the range of the Y-axis is set to the magnitudes of the other PCs.

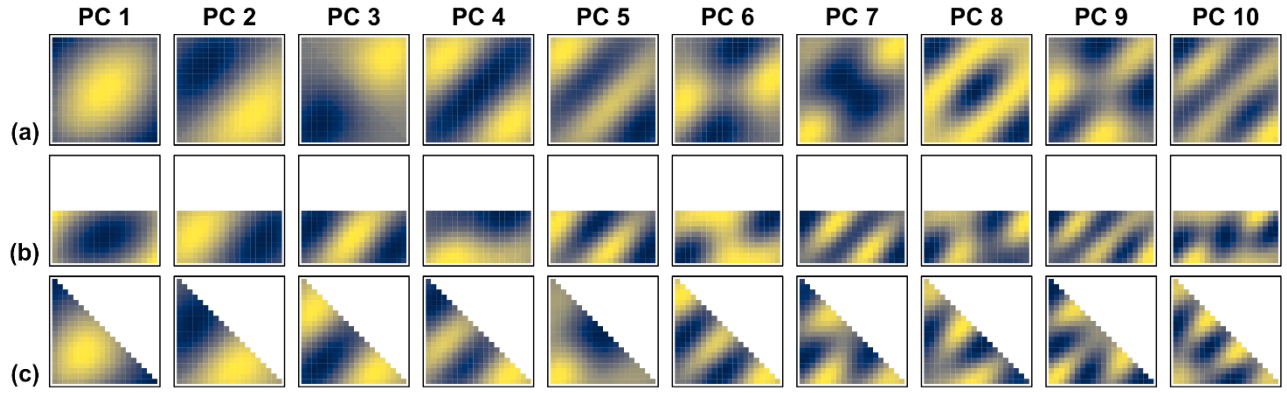

Figure S9 Anisotropic example: Overview of the ten leading DD reference patterns for anisotropic spatial correlation with a direction (angle) of 45° clockwise from North and an anisotropy ratio of 2 with the longer spatial correlation length being 10 cells, and the domain boundaries (a) square, (b) rectangle and (c) triangle from Figure 6. All cells within the boundaries were used. The patterns were estimated with the stochastic method from ensembles with 100 data sets, each with time series length 10 000, using and anisotropic exponential covariance model. In each subplot, the colour gradient depicts from blue to yellow the range between the minimum and maximum values of the respective spatial pattern.

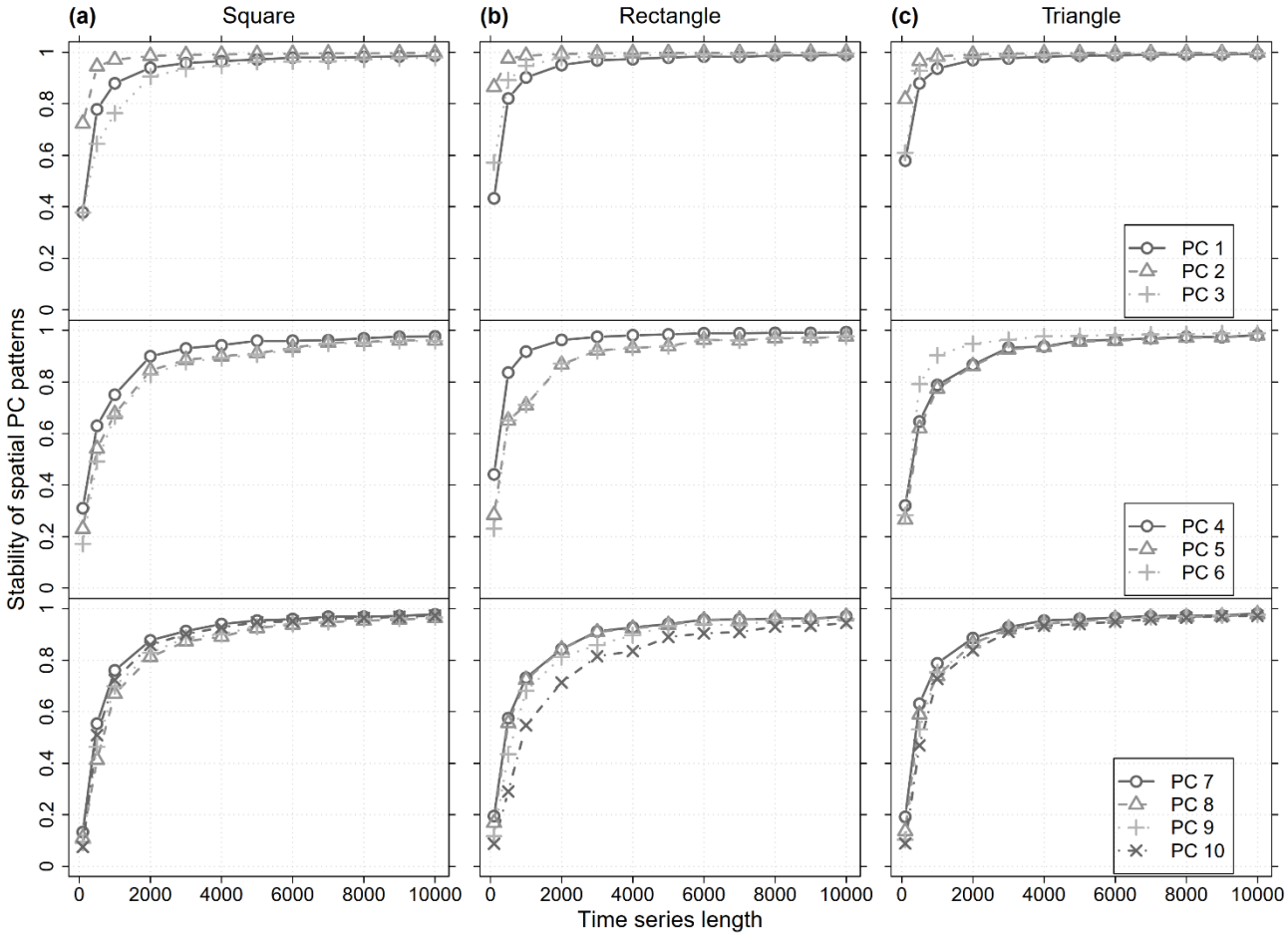

Figure S10 Stability of the spatial PC patterns as in Figure 7 but for the patterns of the anisotropic example from Figure S9. The stability is measured by the mean R^2 of the correlation between the spatial patterns of all PCs with identical rank derived from an ensemble of 100 data sets simulated with the respective time series length. For details see the caption of Figure 7. The spatial correlation properties used in the simulation of the data are described in the caption of Figure S9.

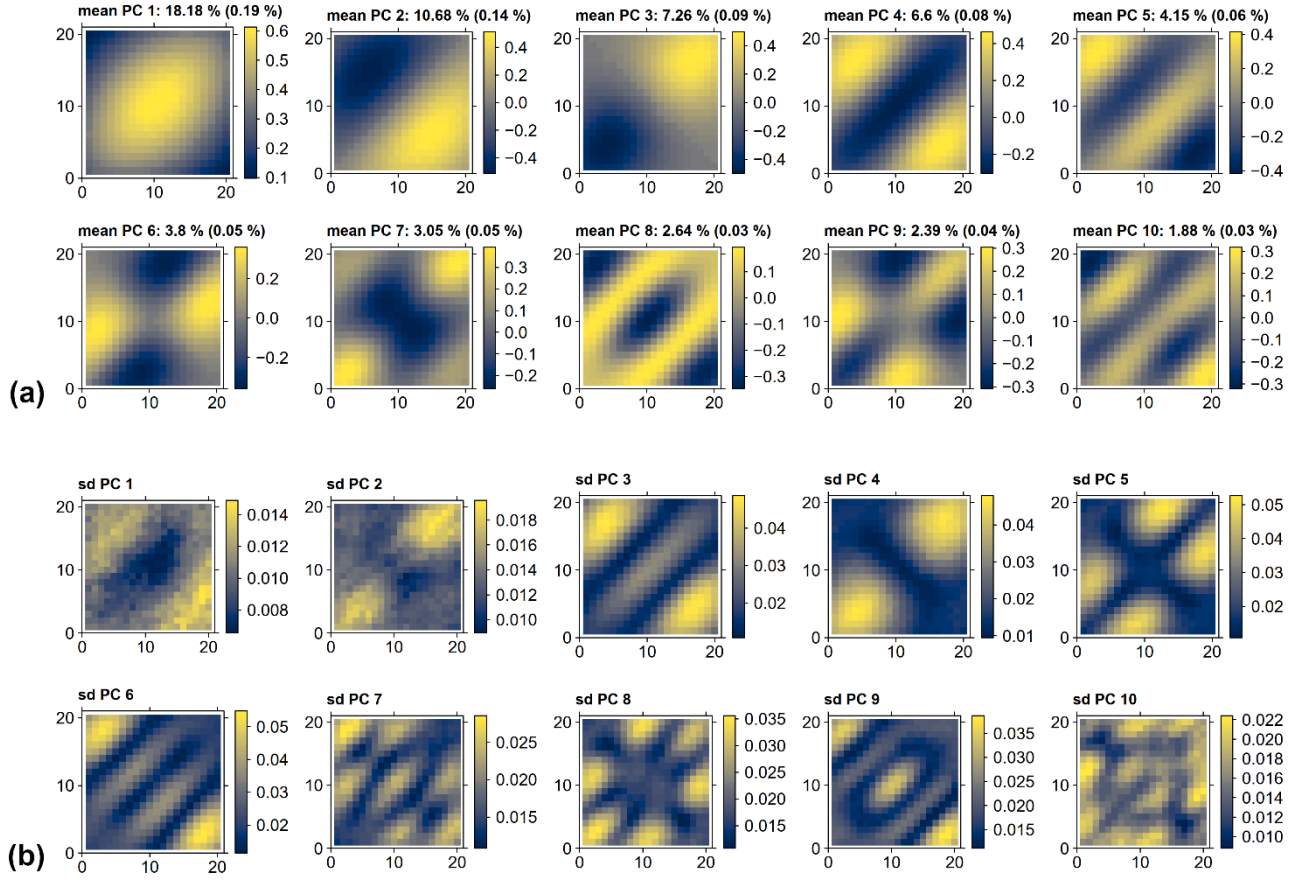

Figure S11 Detail plot of mean (a) and standard deviation (b) of the spatial patterns from the leading ten PCs of the data set ensemble with the square domain shown in Figure S9a. The mean (and standard deviation) of the percentages of variance assigned to the respective PCs from the 100 PCAs of the ensemble is given in the panel titles of (a).

	2rPCs		3rPCs			4rPCs			
	rPC 1	rPC 2	rPC 1	rPC 2	rPC 3	rPC 1	rPC 2	rPC 3	rPC 4
Square	0.68	0.58	0.69	0.62	0.64	0.65	0.61	0.66	0.58
Rectangle	0.56	0.5	0.59	0.57	0.54	0.64	0.55	0.51	* 0.55
Triangle	0.53	0.55	0.59	0.63	0.53	* 0.52	0.63	0.59	0.54

Table S2 Contrasts (differences between minimum and maximum) of the varimax rotated spatial PC patterns from the precipitation PCAs (Figure 17). Most rotated patterns exhibited either only negative loadings or only positive loadings. Patterns with both positive and negative loadings are marked with *.

	PC 1	PC 2	PC 3	PC 4	PC 5	PC 6	PC 7	PC 8	PC 9	PC 10
Square	0.24	0.82	0.70	0.53	0.51	0.46	0.36	0.30	0.30	0.42
Rectangle	0.19	0.69	0.59	0.44	0.38	0.36	0.43	0.32	0.26	0.31
Triangle	0.17	0.75	0.67	0.49	0.37	0.37	0.33	0.35	0.32	0.29

Table S3 Contrasts (differences between minimum and maximum) of the unrotated spatial PC patterns from the precipitation PCAs (Figure 16). Except from the patterns of PC 1, all patterns exhibited positive and negative loadings.